Sensitivities of Tropical Cyclones to Surface Friction and the Coriolis Parameter in a 2-d Cloud-resolving Model

Winston C. Chao[1], Baode Chen[2] and Wei-Kuo Tao[1]

Popular summary

Submitted to Journal of the Atmospheric Sciences

The sensitivities to surface friction and the Coriolis parameter in tropical cyclogenesis are studied using an axisymmetric version of the Goddard cloud ensemble model. The Coriolis parameter is related to earth's rotation rate and the latitude. Our experiments demonstrate that tropical cyclogenesis can still occur without surface friction. However, the resulting tropical cyclone has very unrealistic structure. Surface friction plays an important role of giving the tropical cyclones their observed smaller size and diminished intensity. Sensitivity of the cyclogenesis process to surface friction, in terms of kinetic energy growth, has different signs in different phases of the tropical cyclone. Only in the brief initial onset phase can increase surface friction yields faster kinetic energy growth. Contrary to the previous theory of Ekman pumping efficiency, which implies a preference for the highest Coriolis parameter in the growth rate if all other parameters are unchanged, our experiments show no such preference.

[1]NASA/Goddard Space Flight Center
[2]GEST Center, University of Maryland at Baltimore County

Sensitivities of Tropical Cyclones to Surface Friction and the Coriolis Parameter in a 2-d Cloud-resolving Model

Winston C. Chao, Baode Chen[1] and Wei-Kuo Tao

NASA/Goddard Space Flight Center, Greenbelt, MD

[1]GEST Center, University of Maryland at Baltimore County, Baltimore, MD

(To be submitted)

Corresponding Author Address
Mail Code 913
NASA/Goddard Space Flight Center
Greenbelt, MD 20771

(301) 614-6242
(301) 614-6307 (fax)
Winston.chao@gsfc.nasa.gov

Abstract

The sensitivities to surface friction and the Coriolis parameter in tropical cyclogenesis are studied using an axisymmetric version of the Goddard cloud ensemble model. Our experiments demonstrate that tropical cyclogenesis can still occur without surface friction. However, the resulting tropical cyclone has very unrealistic structure. Surface friction plays an important role of giving the tropical cyclones their observed smaller size and diminished intensity. Sensitivity of the cyclogenesis process to surface friction, in terms of kinetic energy growth, has different signs in different phases of the tropical cyclone. Contrary to the notion of Ekman pumping efficiency, which implies a preference for the highest Coriolis parameter in the growth rate if all other parameters are unchanged, our experiments show no such preference.

3. Introduction

Conditional instability of the second kind (CISK) (Ooyama 1964 and Charney and Eliassen 1964; hereafter CE), had till not long ago been a popular concept in interpreting tropical cyclogenesis. Its variant, the frictional wave-CISK, has been a contender in the recent years in interpreting the Madden-Julian oscillation (e.g., Wang 1988, Xie and Kubokawa 1990.) Recently these ideas have come under criticism. Foremost among the critics are Emanuel, Neelin, and Bretherton (1994). They pointed out that in CISK the external view of the convective heating is implied; that is convective heating is specified without the quasi-equilibrium consideration. Among the other critics, Craig and Gray (1996) demonstrated in a numerical model of tropical cyclone (TC) that CISK does not work as well as another contending theory, the wind-induced surface heat exchange (WISHE, Emanuel et al. 1994) theory, in the sense that the intensification rate was found to be relatively insensitive to the frictional drag coefficient. This paper does not intend to assess the recent developments related to CISK. Instead, it focuses on two other aspects of CISK.

The CISK theory has two prominent features. One is the important role assigned to surface friction. In the CISK theory the low-level convergence is induced by surface friction, implying that surface friction is necessary for TC. Also according to the CISK theory (Charney and Eliassen 1964), surface friction plays a dual role in the sense that besides its damping role it, through the frictionally induced low-level convergence, also brings in moisture and thus plays an energy enhancing role. The other prominent feature is the idea of Ekman pumping (which is another name for the frictionally-induced low-

level convergence) efficiency (Charney 1971, 1973), which yields a TC growth rate proportional to the Coriolis force. In this paper these two features will be examined by focusing on the sensitivities of TC to surface frictional coefficient and the Coriolis parameter using an axisymmetric cloud-resolving model.

2. Experimental setup

The model used is an axisymmetric version of the latest version of the Goddard cloud ensemble model (Tao et al. 2002). An earlier version of this model was documented in Tao and Simpson (1993). The model variables include 3d velocity, potential temperature, perturbation pressure, turbulent kinetic energy and mixing ratios of all three water phases. An important feature of this type of models is that, since individual clouds are resolved, no cumulus parameterization is used. Therefore, unlike the meso-scale models, the success of this model does not depend on cumulus parameterization. However, the realism of the model still depends on the quality of the microphysics and turbulence parameterizations. Also the limitations of the 2-d structure, such as the lack of interaction between (azimuthal) mean flow and eddies, should be acknowledged. The model has 33 stretched vertical grids, which vary from 30 m near the bottom to 1140 m near the top. The vertical domain is about 21 km. The horizontal domain covers a radius of 924 km (770 grids) with a grid size of 1.25 km. The time step is 10 seconds. An open lateral boundary condition is used. The sea surface temperature is specified at 29°C. Unless specified otherwise, the Coriolis parameter is set at its value at 15°N. The surface fluxes are computed by the bulk scheme developed by Liu et al.

(1979). The Newtonian cooling is used with a time scale of 12 hours. The reference vertical temperature profile used in the Newtonian cooling is that of Jordan (1958). The Newtonian cooling models not only the effect of radiative processes (which would require the use of radiative equilibrium temperature profile as the reference profile toward which the temperature profile is relaxed to) but also the effect of processes with scale larger than that of TC. Our experiments showed that if the Newtonian cooling is replaced by the radiation package that exists in the original 2D model (short wave parameterization developed by Chou and Suarez (1999) and long wave parameterization developed by Chou et al. (1995), Chou and Kouvaris (1991), Chou et al. (1999) and Kratz et al. (1998)) that simulates radiative processes only (see Tao et al. 2002 for description, the simulated TC is slightly stronger. Other authors have also obtained reasonable simulation of TC with full radiation package (e. g., Craig 1996). However, the use of full radiation package doubles the use of computer time for the model, we thus decided to proceed with the TC simulation with the Newtonian cooling.

The initial condition has a temperature uniform in the radial direction and its vertical profile is that of Jordan (1958). The initial winds are a weak vortex in the tangential winds superimposed on a resting atmosphere. That is:

$$v = \max(0., v_1),\ v_1 = (\frac{v_{max}}{r_{max)}})\ r\ \exp(1. - \frac{r}{r_{max}})(1. - \frac{z}{z_T})$$

where v_{max}= 10 m/s, r_{max}=105 km, and z_T=16 km. The initial sea level pressure is set at 1002 hPs everywhere. Since there is no surface pressure perturbation, the initial condition is not in gradient balance. This initial condition (along with the other model

settings) is enough to lead to cyclogenesis, but the initial stage (say, the first 24 hrs) is not considered to resemble anything observed. An initial condition that is in gradient wind balance would have a surge of upward motion at the center due to the Ekman pumping at the start of the integration (as surface friction reduces the Coriolis force, the difference between the pressure gradient force and the sum of the Coriolis force and the centrefugal force pushes the air in the boundary layer toward the center), which does not resemble anything observed either. A more satisfactory initial condition should have a balance among pressure gradient force, the Coriolis force, the centrifugal force, and surface friction; but that is more difficult to specify. Our initial condition avoids the initial artificial upward motion associated with the balanced gradient wind initial condition; thus the possibility of genesis being set off by the initial condition is avoided.

The control experiment reaches quasi-equilibrium after about 10 days with an eye-wall extending from 15 to 35 km radius. Fig. 1 shows the results averaged over the 24-hour period ending day 15 hr 0, which are reasonable in comparison with the observations. The maximum tangential wind of more than 65 m/s is located at about 20 km radius at the top of the boundary layer. The minimum sea level pressure is about 955 hPa. The maximum precipitation rate reaches more than 110 mm/hr. The warm core temperature perturbation reaches more than 12°C. Thus the overall simulation is deemed successful and the model is considered adequate for our experiments. None of our experiments has shown eye-wall replacement.

3. Sensitivity experiments

Sensitivity to surface friction

Three experiments identical to the control but with zero, half and double surface drag coefficient were done. The experiment without surface friction has also obtained the cyclogenesis process. Thus, surface friction is not a necessary condition for cyclogenesis or for the mature TC. However, without surface friction the TC has a very unrealistic structure. Fig. 2 shows the results averaged over the 24-hour period ending at day 15 hr 0. The eye-wall in this case is quite far (about 70 km) from the center. The maximum tangential wind reaches 50 m/s at around 70km from the center. This maximum wind speed is weaker than that in the control experiment. However, since it occurs at a larger radius, it provides more kinetic energy. Unlike the control experiment, the maximum tangential wind is not very close to the surface. The converging flow toward the eye-wall obviously can exist without the presence of surface friction. However this converging flow is not confined in the low-levels. This experiment supports one of the central ideas of CISK that the low-level convergence in the tropical cyclone is induced by surface friction. In other words, surface friction is necessary for the existence of low-level convergence. Moreover, surface friction is important in giving the TC its observed smaller size and weaker intensity. The sensitivity of the low-level convergence to surface friction will be examined shortly. Without surface friction to reduce surface wind speed the converging air cannot reach very close to the center, resulting in an eye-wall with a large radius. This is due to the fact that the converging low-level air, in the absence of surface friction, gains high enough tangential wind at large radius to yield high outward centrifugal force and Coriolis force to prevent air from getting close to the center (i. e., to counter the pressure gradient force.)

In the experiments with double and half surface friction coefficients the results show that higher surface friction renders a smaller and weaker TC but with earlier and more intense cyclogenesis process in terms of minimal sea level pressure (Fig. 3). Since the sea level pressure drop at the TC center depends on the cancellation between the upper-level divergence and the low-level convergence and, as will be soon shown, higher surface friction leads to higher low-level convergence and the more intense cyclogenesis process helps evacuate air from the TC center leading to a more rapid sea level pressure drop. Similar to what was obtained by Craig and Gray (1996) using a modified Rotunno and Emanuel (1987) model, the growth rate of the tropical cyclogenesis processes is not very sensitive to the surface friction if the minimum sea level pressure is used as a measure. Fig. 3a shows that the minimum sea level pressure drops at about the same rate for all the cases. However, if the growth rate is measured in terms of total kinetic energy in the model domain, there is sensitivity to the surface friction. Fig. 3b shows that the growth rate of total kinetic energy, divided by the horizontal area of the model, is higher when surface friction is smaller. Specifically, all three (control, half and double) experiments reach about the same amount kinetic energy at hr 120 and the onset time is latest for the lowest surface friction case.

Thus far we have shown that surface friction is important for low-level convergence and for a realistic simulation of TC. To further study the role of surface friction in TC, we need more experiments. In another series of experiments the results of the control run at hrs 48, 96 and 240 (the incipient, growing, and mature phases) are used as the initial conditions for integrations of one day duration with half and double surface drag coefficient. Fig. 4.a shows the minimum sea level pressure of these experiments. It

reveals that in the 24 hour period starting from hr 48 (the incipient stage) doubling surface friction leads to a more rapid decrease of the minimum sea level pressure. Fig. 5.a shows the 24 hr averaged boundary layer (bottom 1 km) mass convergence for the control, half and double surface friction cases as functions of radius for these experiments. Apparently, higher surface drag increases the low-level convergence in all phases of the TC development. The increase in the low-level convergence is accompanied by an increase in the precipitation rate (Fig. 5.b). In the 24 hour period starting hr 48 increasing surface friction leads to a faster minimum sea level pressure drop and a faster growth of total kinetic energy (Fig. 4.b). In the 24 hour periods starting from hr 96 (in the rapid intensification period) and hr 240 (in the mature stage) increasing surface drag also leads to an increase in low-level convergence but a slower drop of the central sea level pressure. The low-level convergence increase is the result of the reduction of the azimuthal wind and thus the reduction of the radially outward Coriolis force and centrifugal force to oppose the pressure gradient force. In the same periods increasing surface drag has decreased the total kinetic energy.

These experiments reveal that the response of the cyclone to surface drag changes, in terms of minimum sea level pressure and total kinetic energy, varies according to the developmental stage of the cyclone; but the response in the low-level convergence does not vary. Thus the Ekman pumping concept, which states that low-level convergence is related to surface friction and which implies that low-level convergence increases when the drag coefficient is increased, appears to be valid. However, increased Ekman pumping yields faster TC growth only in the incipient phase. This is consistent with the finding that higher surface friction leads to earlier onset of the

genesis process (Fig. 3.a). Although higher surface friction can lead to earlier onset in terms of sea level pressure, it leads to higher area averaged kinetic energy only in the short early hours (Fig. 3.b). Therefore surface friction does play a dual role (the traditional energy damping role and the role of inducing moisture convergence in the boundary layer which supply latent energy to the core). However, with the minor exception in the early hours the net effect of higher surface friction is still to remove more kinetic energy from the system.

Sensitivity to the Coriolis parameter

Fig. 6 shows the minimum sea level pressure as a function of time for experiments with various values of the Coriolis parameter corresponding to various latitudes (while keeping everything else the same.) It shows that all experiments reach a minimal sea level pressure of about 930 hPa, but the onset is earlier for lower Coriolis parameter. The peak growth rate tends to become smaller with increasing Coriolis parameter. However, the minimum sea level pressure is not necessarily the only measure of the TC intensity. Fig. 7 shows the total kinetic energy, divided by the area of the model horizontal domain, of these experiments. It also shows that higher Coriolis parameter gives later onset. The maximum total kinetic energy that is attained depends on the Coriolis parameter. For values of the Coriolis parameter that corresponds to latitudes lower than 30N, the higher the Coriolis parameter the larger the maximum kinetic energy. For other values of the Coriolis parameter the maximum total kinetic energy does not very much depend on the Coriolis parameter. The maximum growth rate in terms of total kinetic energy increase appears to occur for the case of Coriolis

parameter corresponding to that of 35N. This figure also shows that the rates of total kinetic energy growth during the period of fastest growth are not very different between 35° and 60° of latitude. At 90° the TC takes longer to reach its maximum total kinetic energy than at the latitudes between 35 and 60. Fig. 8 shows the precipitation rate averaged over day 10 to day 15 for various f values (their corresponding latitudes). The most optimal latitude for precipitation appears to be 20N in terms of total precipitation, eye-wall size and intensity. Below 30N the radius of the eye-wall increases as the latitude is raised (in computing f); whereas above 30N there is no strong dependency. These results do not support the Ekman pumping efficiency idea of Charney (1973) in interpreting the TC growth, which yields an optimal latitude at the poles in terms of growth rate for these experiments. The Coriolis parameter has two effects on the tropical cyclone. First, it provides inertial stability, which suppress convection and therefore the TC itself. This can be understood through the equivalence between f and vertical stability (Chao and Chen 2001). Second, the Coriolis parameter also generates azimuthal wind, which enhances the surface wind speed and thus evaporation. These two effects oppose each other in determining the optimal latitude. The former attracts the TC towards the equator and the latter towards the higher latitudes (i.e. the poles).

4. Summary

In summary, in this work we have examined the sensitivities of tropical cyclones in an axisymmetic cloud-resolving model to surface friction and the Coriolis parameter. Although the tropical cyclogenesis process can occur without surface friction, the

developed TC is very unrealistic. Without surface friction the radius of the eye-wall is as large as 70 km and the maximum precipitation rate is more than one order of magnitude less. The total kinetic energy is much greater but the minimum surface pressure is much higher. Also the strongest inflow is not at the low-levels. Surface friction gives the TC the observed smaller size, and lower intensity. It also confines the inflow in the boundary layer. Further experiments with varying surface friction coefficients reveal that with higher surface friction coefficient cyclogenesis occurs sooner and faster but it terminates sooner also, giving a weaker TC. In all phases of the cyclogenesis process higher surface friction giving higher boundary layer convergence. However the responses in minimum sea level pressure and total kinetic energy are different in different phases. In the very beginning phase of the cyclogenesis, higher surface friction leads to faster drop of the minimum sea-level pressure and an increase in total kinetic energy, just the opposite to what happens in the later phases. Our study also shows that contrary to the Ekman pumping efficiency idea in the interpretation of TC growth, which prefers the highest value for f, tropical cyclogenesis process has a different preferred value for f, its value at 35N if measured in terms of fastest rate of drop of the minimum sea level pressure and in terms of fastest growth of total kinetic energy that is attained during the cyclogenesis processes (Figs. 6 and 7).

References

Charney, J. G., 1971: Tropical cyclogenesis and the formation of the ITCZ. *Mathematical Problems of Geophysical Fluid Dynamics.* W. H. Reid, Ed., Lectures in Applied Mathematics, Vol. 13. *Amer. Math. Soc.*, 355-368.

Chao, W. C., and B. Chen, 2001: Multiple quasi-equilibria of the ITCZ and the origin of monsoon onset. Part II. Rotational ITCZ attractors. *J. Atmos. Sci.* **58**, 2820-2831.

Charney, J. G. and A. Eliassen, 1964: On the growth of the hurricane depression. *J. Atmos. Sci.*, **21**, 68-75.

Chou, M. D. and L. Kouvaris, 1991: Calculations of transmission functions in the IR CO2 and O3 Bands. *Geophys. Res.*, **96**, 9003-9012.

Chou, M. D., W. Ridgway, and M.-H. Yan, 1995: Parameterizations of water vapor IR radiation transfer in both the middle and lower atmospheres. *J. Atmos. Sci.*, **52**, 1159-1167.

Chou, M. D., K. T. Lee, S. C. Tsay, and Q. Fu, 1999: Parameterization for cloud longwave scattering for use in atmospheric models. *J. Climate*, **12**, 159-169.

Chou, M. D. and M. J. Suarez, 1999: A shortwave radiation Parameterization for Atmospheric studies. NASA/TM-104606. pp 40.

Craig, G. C., 1996: Numerical experiments on radiation and tropical cyclones. *Q. J. R.. Meteoroi. Soc.*, **122**, 415-422.

Craig, G. C. and S. L. Gray, 1996: CISK or WISHE as the mechanism for tropical cyclone intensification. *J. Atmos, Sci.*, **53**, 3528-3540.

Emanuel, K. A., J. D. Neelin and C. S. Bretherton, 1994: On large-scale circulations in convecting atmospheres. *Q. J. Roy. Met. Soc.*, **120**, 1111-1143.

Jordan, C. L., 1958: Mean soundings for the west Indies area. *J. Atmos. Sci.*, **15**, 91–97.

Kratz, D. P., M. D. Chou, M. M.-H. Yan, and C.-H. Ho, 1998: Minor trace gas radiative forcing calculation using the k-distribution method with one-parameter scaling. *J. Geophy. Res.* **103**, 31647-31656.

Liu, W. T., K. B. Katsaro, and J. A. Businger, 1979: Bulk parameterization of the air-sea exchange of heat and water vapor including the molecular constraints at the interface. *J. Atmos. Sci.*, **36**, 1722-1735.

Rotunno, R., and K. A. Emanuel, 1987: An air-sea interaction theory for tropical cyclones. Part II. *J. Atmos. Sci.*, **44**, 542-561.

Tao, W.-K. and J. Simpson, 1993: Goddard cumulus ensemble model. Part I: Model description. *TAO*, **4**, 35-72.

Tao. W.-K., J. Simpson, D. Baker, S. Braun, M.-D. Chou. B. Ferrier, D. Johnson, A. Khain, L. Lang. B. Lynn, C.-L. Shier, D. Starr, C.-H. Sui, Y. Wang and P. Wetzel, 2002: Microphysics, Radiation and surface processes in the Goddard cumulus ensemble (GCE) model. *Meteor. and Atmos. Phys.* In press.

Wang, B., 1988: Dynamics of tropical low-frequency waves: An analysis of the moist Kelvin wave. *J. Atmos. Sci.*, **45,** 2051-2065.

Xie, S.-P. and A. Kubokawa, 1990: On the wave-CISK in the presence of a frictional boundary layer. *J. Meteor. Soc. Japan*, **68**, 651-657.

Figure Caption

Figure 1. Results of the control experiment averaged over the 24 hr period ending at hour 0 of day 15. (a) tangential wind (m/s), (b) radial wind (m/s), (c) vertical velocity (10^{-2} m/s), (d) temperature minus reference temperature (°C), which a function of pressure only, (e) angular momentum (m2s-1), (f) potential vorticity (10^{-6} m^2 kg^{-1} s^{-1}) as functions of height and radius, (g) sea level pressure (hPa) as a function of radius, and (h) precipitation (mm/day) as a function of radius.

Figure 2. Same as Figure 1 but for the experiment without surface friction.

Figure 3. (a) Minimum sea level pressure (in hPa) as functions of time for control, half, double and no surface friction.

(b) same as (a) but for total kinetic energy per unit area (in 10^4 J/m^2.)

Figure 4. (a) Minimum sea level pressure (in hPa) as functions of time for the control experiment and for the double and half surface friction experiments for three 24 hour periods starting from the control and (b) same as (a) but for total kinetic energy per unit area (in 10^4 J/m^2.)

Figure 5.a. Mass flux in radial direction in the bottom one kilometer in 10^9 kg/s as functions of radial distance from the TC center for the control and half and double surface friction averaged over the 24 hour period starting (a) hour 48, (b) hour 96 and (c) hour 240.

Figure 5.b. Same as Fig. 5.a but for precipitation rate (in mm/hr).

Figure 6. Minimum sea level pressure (in hPa) as a function of time for various values of the Coriolis parameter, labeled by the corresponding latitude

Figure 7. Same as Fig. 6.a but for total kinetic energy per unit area (in 10^4 J/m^2.)

Figure 8. Same as Fig. 6 but for precipitation rate (mm/day) averaged between day 10 and day 15.

Fig 1

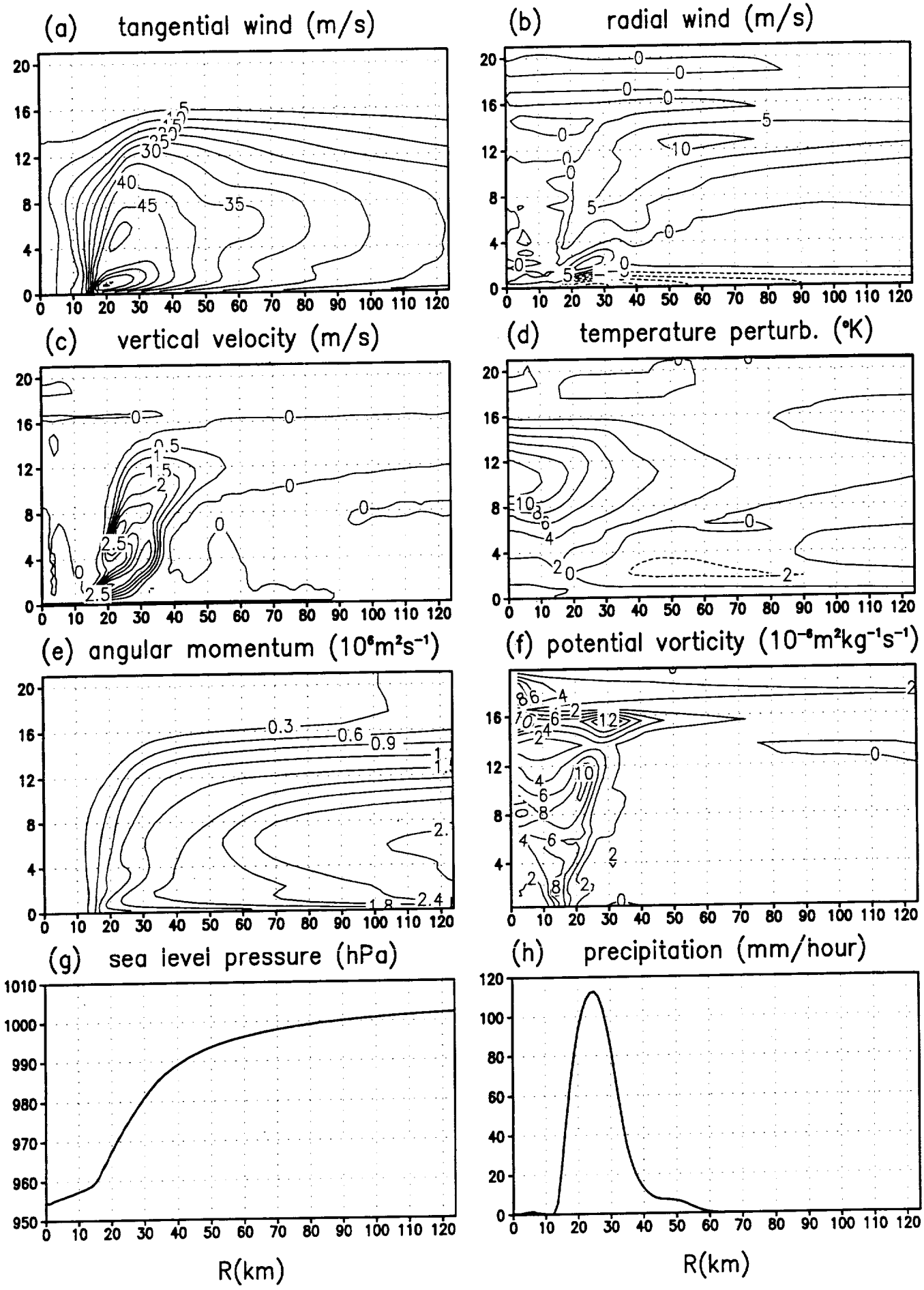
(a) tangential wind (m/s)
(b) radial wind (m/s)
(c) vertical velocity (m/s)
(d) temperature perturb. (°K)
(e) angular momentum ($10^6 m^2 s^{-1}$)
(f) potential vorticity ($10^{-6} m^2 kg^{-1} s^{-1}$)
(g) sea level pressure (hPa)
(h) precipitation (mm/hour)
R(km)
R(km)

Fig 2

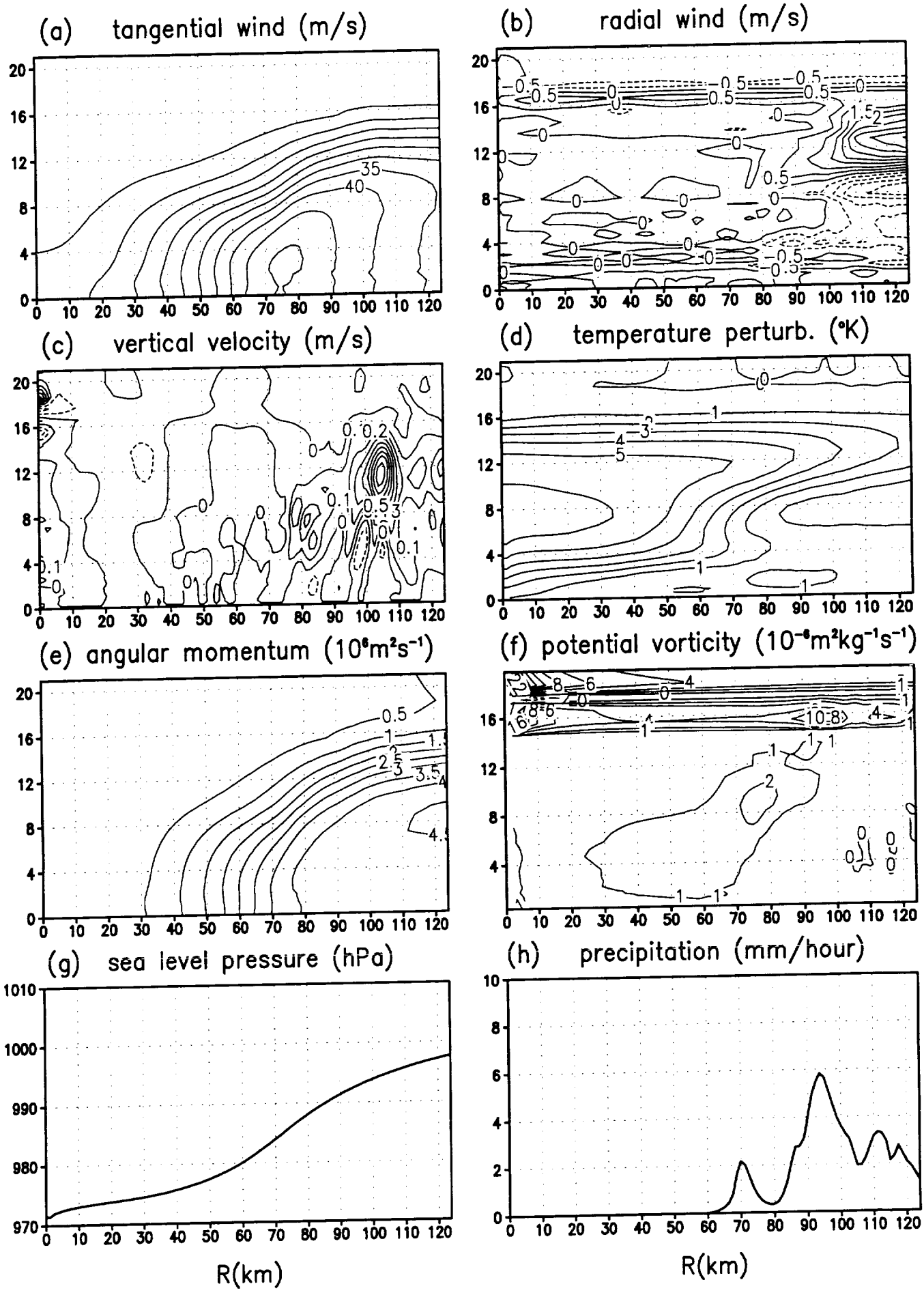
(a) tangential wind (m/s)
(b) radial wind (m/s)
(c) vertical velocity (m/s)
(d) temperature perturb. (°K)
(e) angular momentum ($10^6 m^2 s^{-1}$)
(f) potential vorticity ($10^{-6} m^2 kg^{-1} s^{-1}$)
(g) sea level pressure (hPa)
(h) precipitation (mm/hour)
R(km)
R(km)

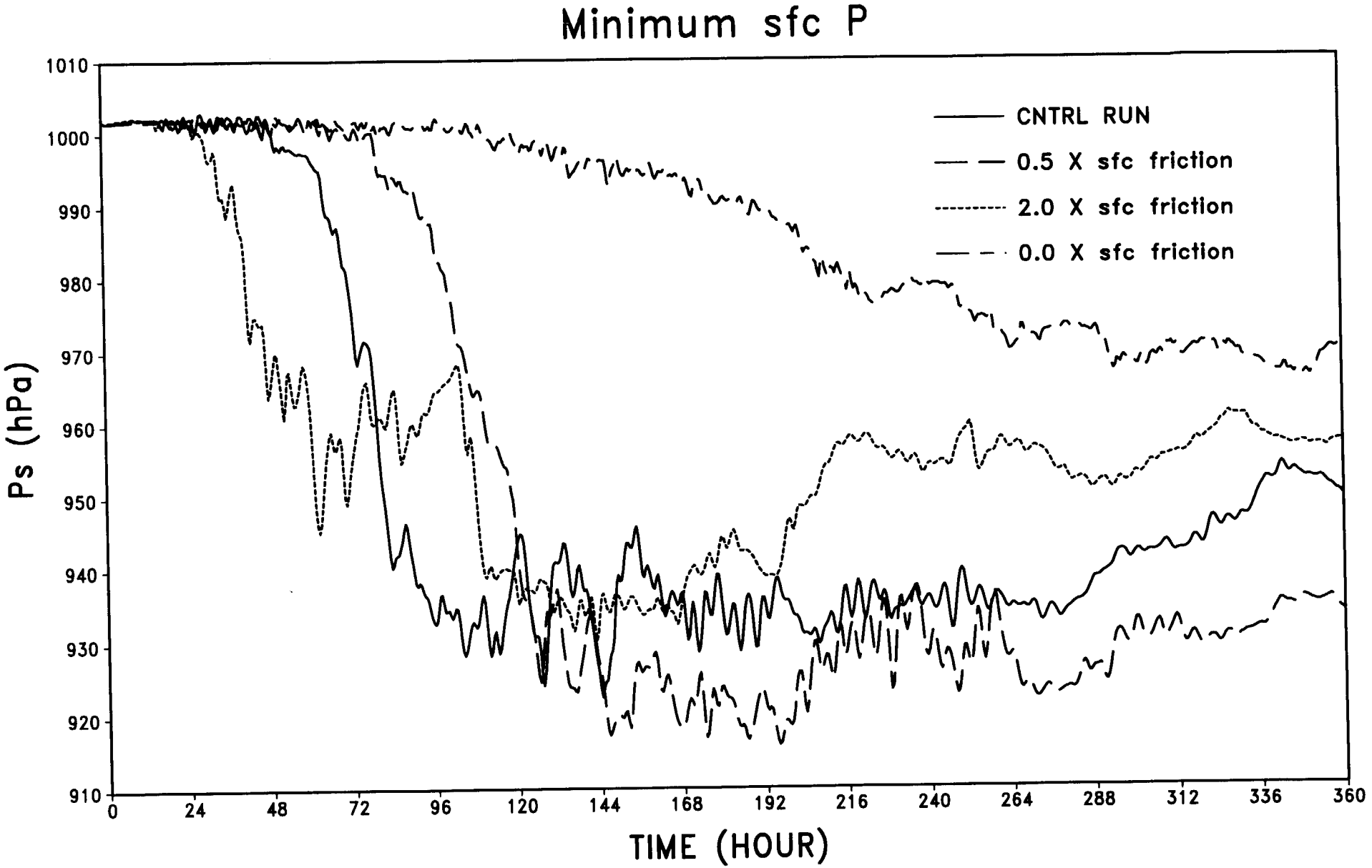
Minimum sfc P
CNTRL RUN
0.5 X sfc friction
2.0 X sfc friction
0.0 X sfc friction
Ps (hPa)
1010
1000
990
980
970
960
950
940
930
920
910
0
24
48
72
96
120
144
168
192
216
240
264
288
312
336
360
TIME (HOUR)

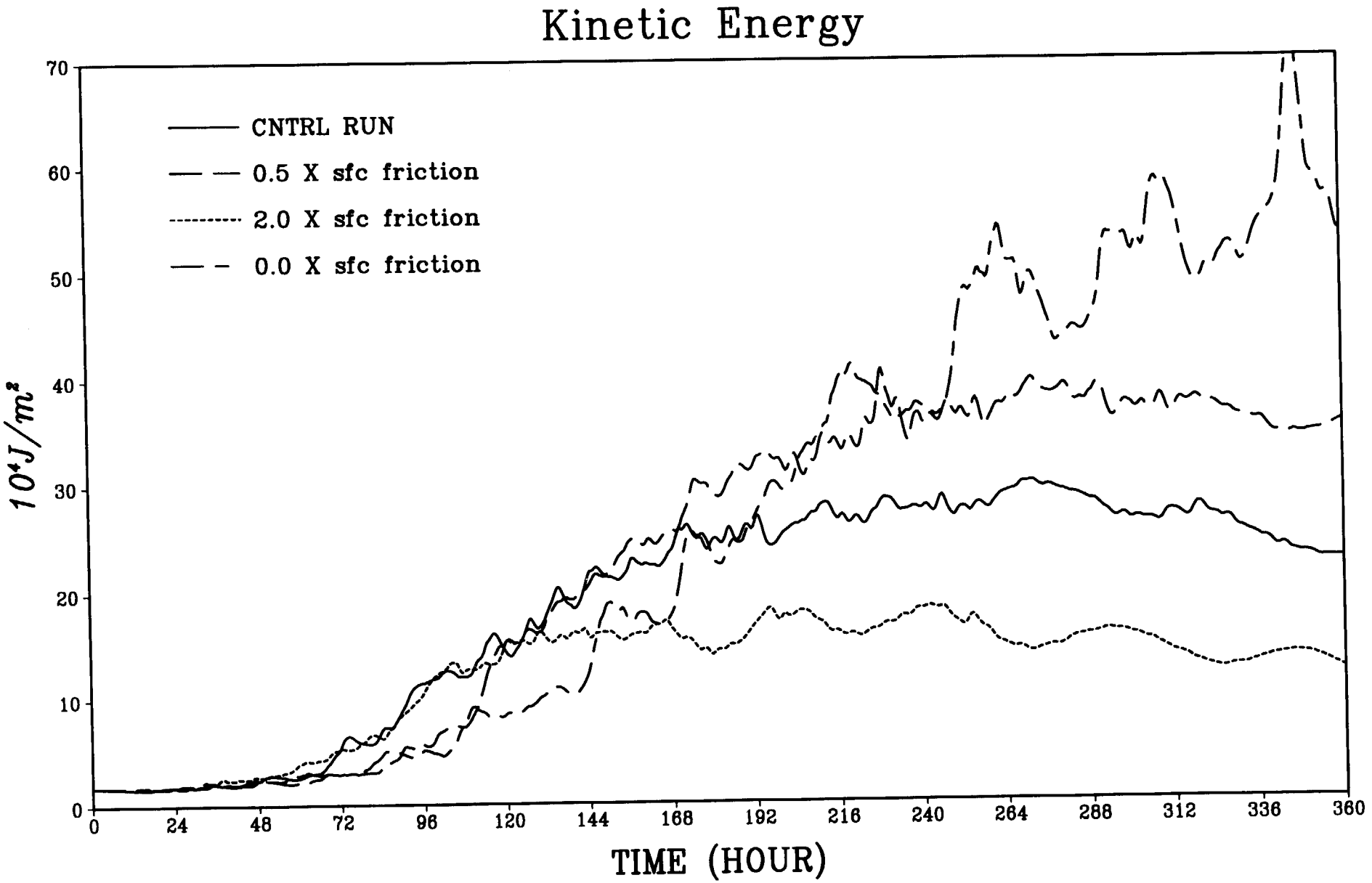
Kinetic Energy
CNTRL RUN
0.5 X sfc friction
2.0 X sfc friction
0.0 X sfc friction
$10^4 J/m^2$
70
60
50
40
30
20
10
0
0
24
48
72
96
120
144
168
192
216
240
264
288
312
336
360
TIME (HOUR)

Fig 4.a

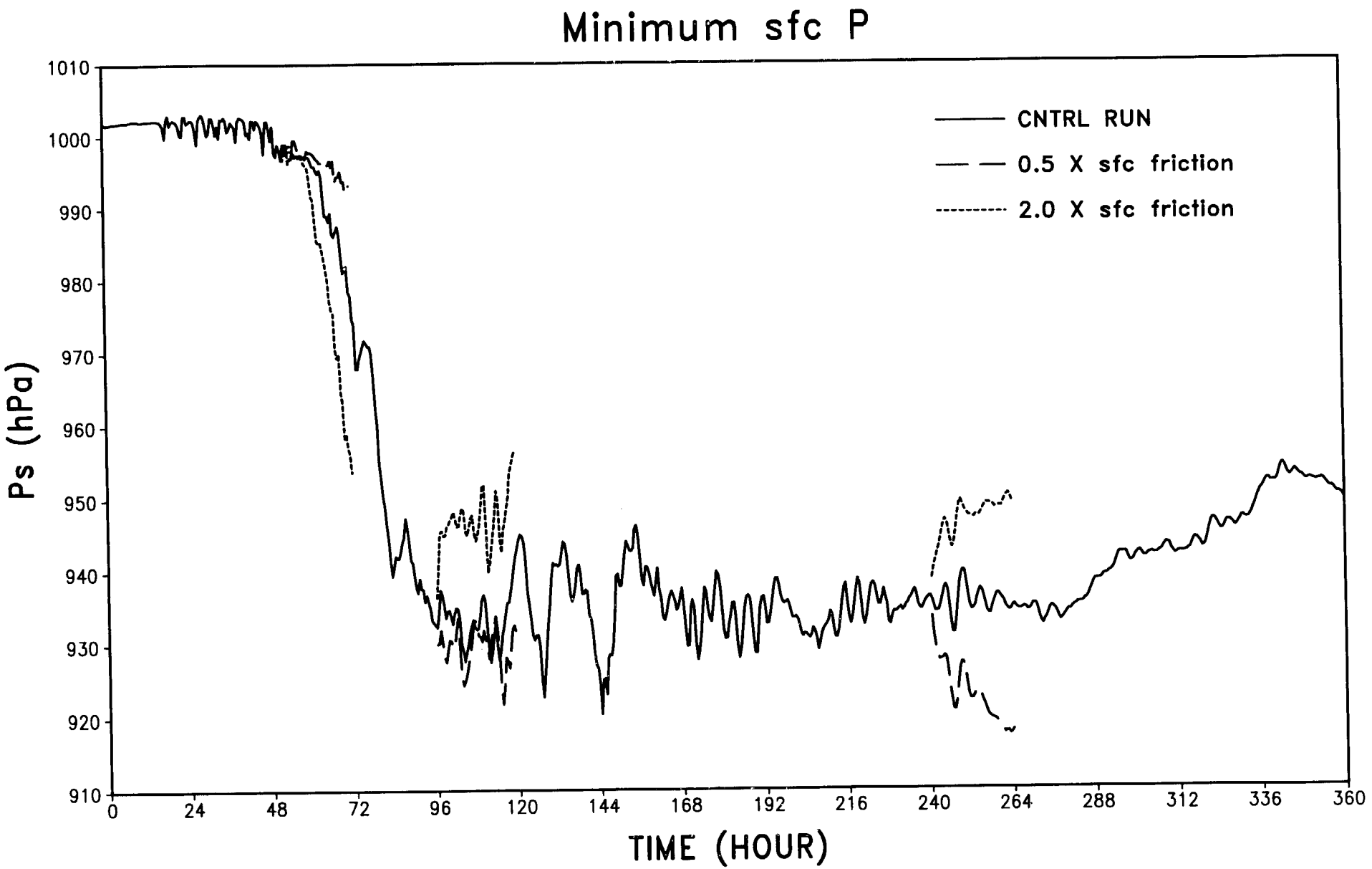
Minimum sfc P
CNTRL RUN
0.5 X sfc friction
2.0 X sfc friction
Ps (hPa)
1010
1000
990
980
970
960
950
940
930
920
910
0
24
48
72
96
120
144
168
192
216
240
264
288
312
336
360
TIME (HOUR)

Fig. 4.6

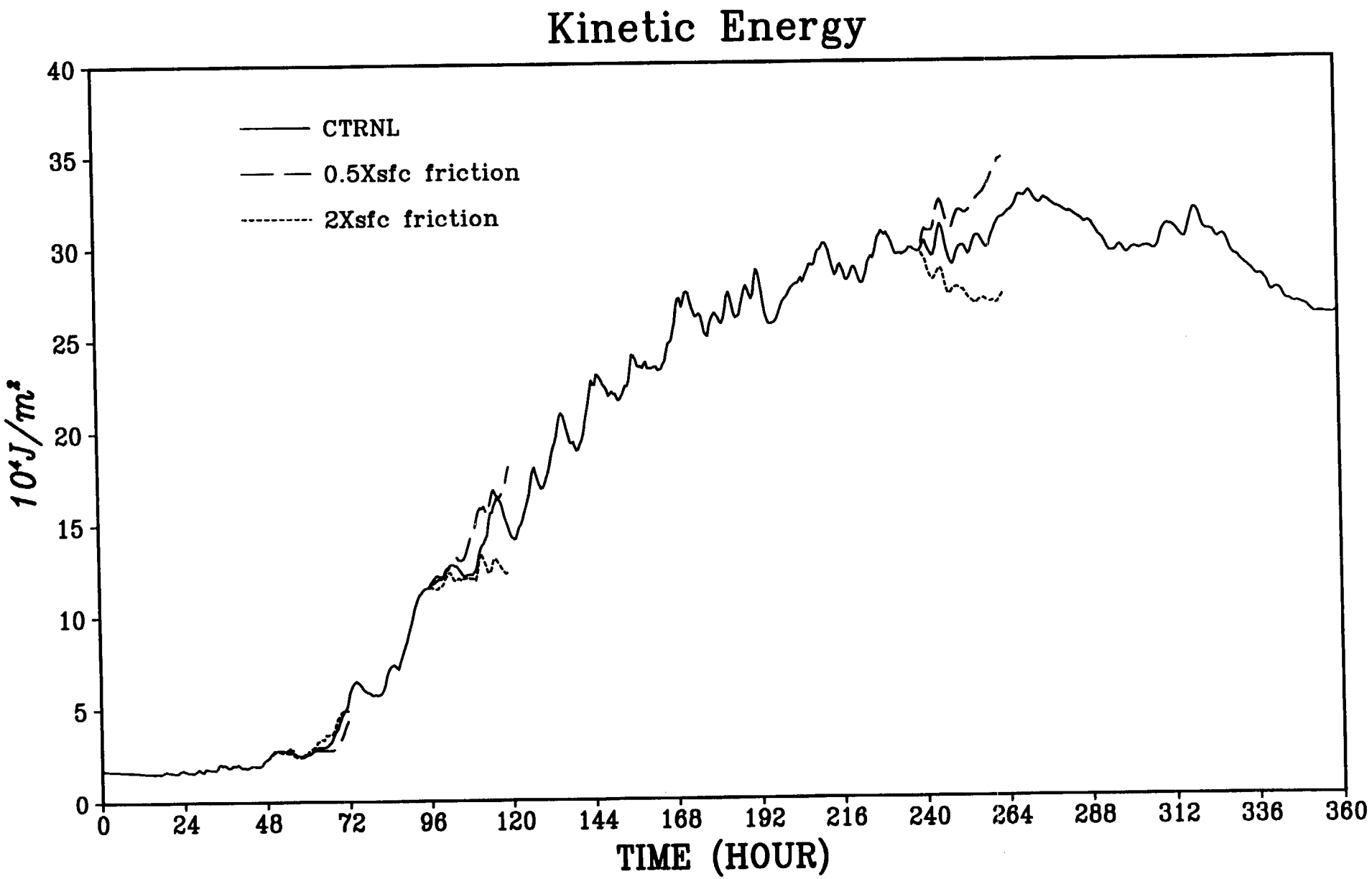
Kinetic Energy
CTRNL
0.5Xsfc friction
2Xsfc friction
$10^4 J/m^2$
0
5
10
15
20
25
30
35
40
0
24
48
72
96
120
144
168
192
216
240
264
288
312
336
360
TIME (HOUR)

Fig 5.a

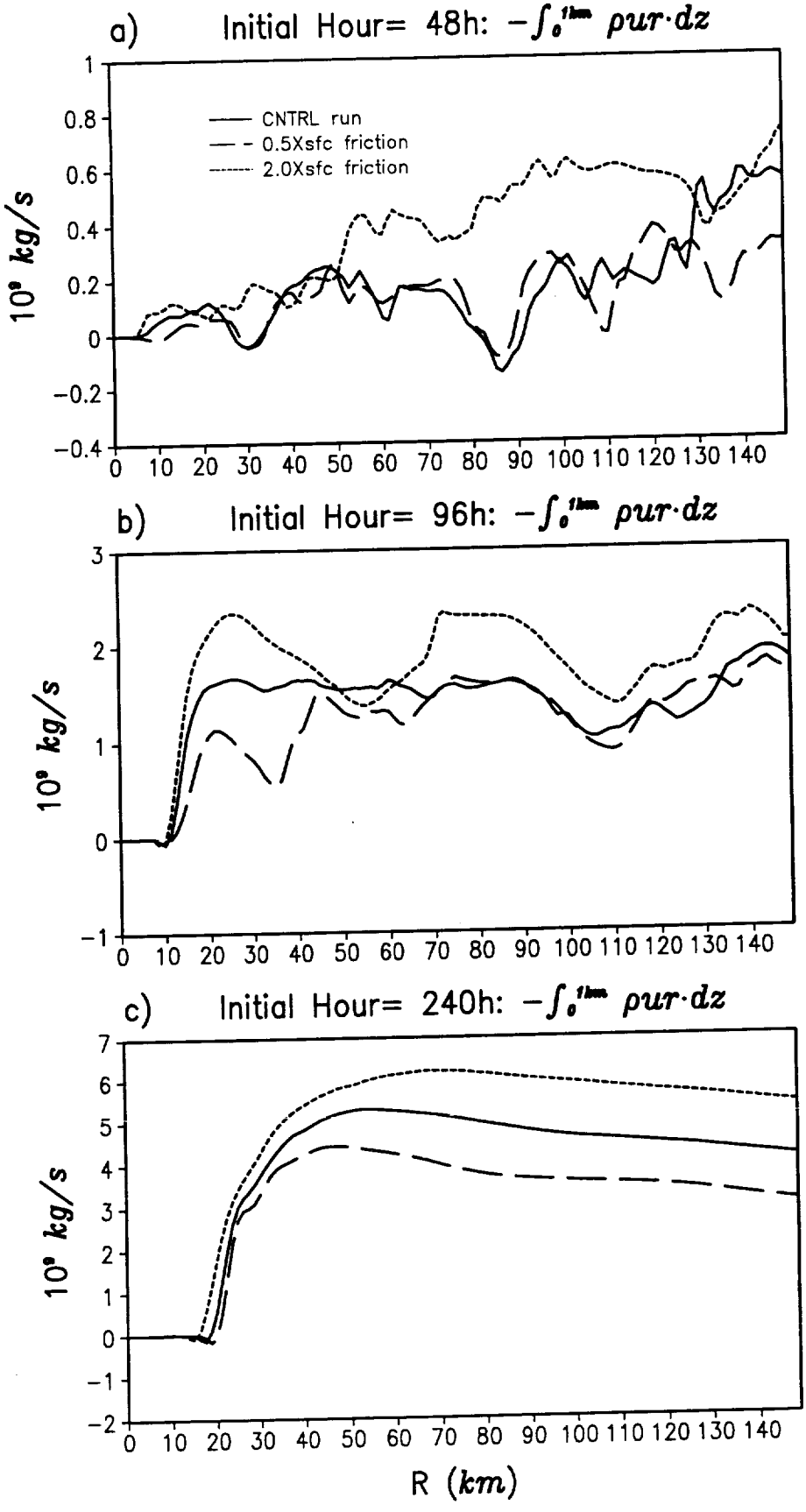
a) Initial Hour= 48h: $-\int_0^{1km} \rho ur \cdot dz$
CNTRL run
0.5Xsfc friction
2.0Xsfc friction
10^9 kg/s
b) Initial Hour= 96h: $-\int_0^{1km} \rho ur \cdot dz$
10^9 kg/s
c) Initial Hour= 240h: $-\int_0^{1km} \rho ur \cdot dz$
10^9 kg/s
R (km)

Fig. 5.6

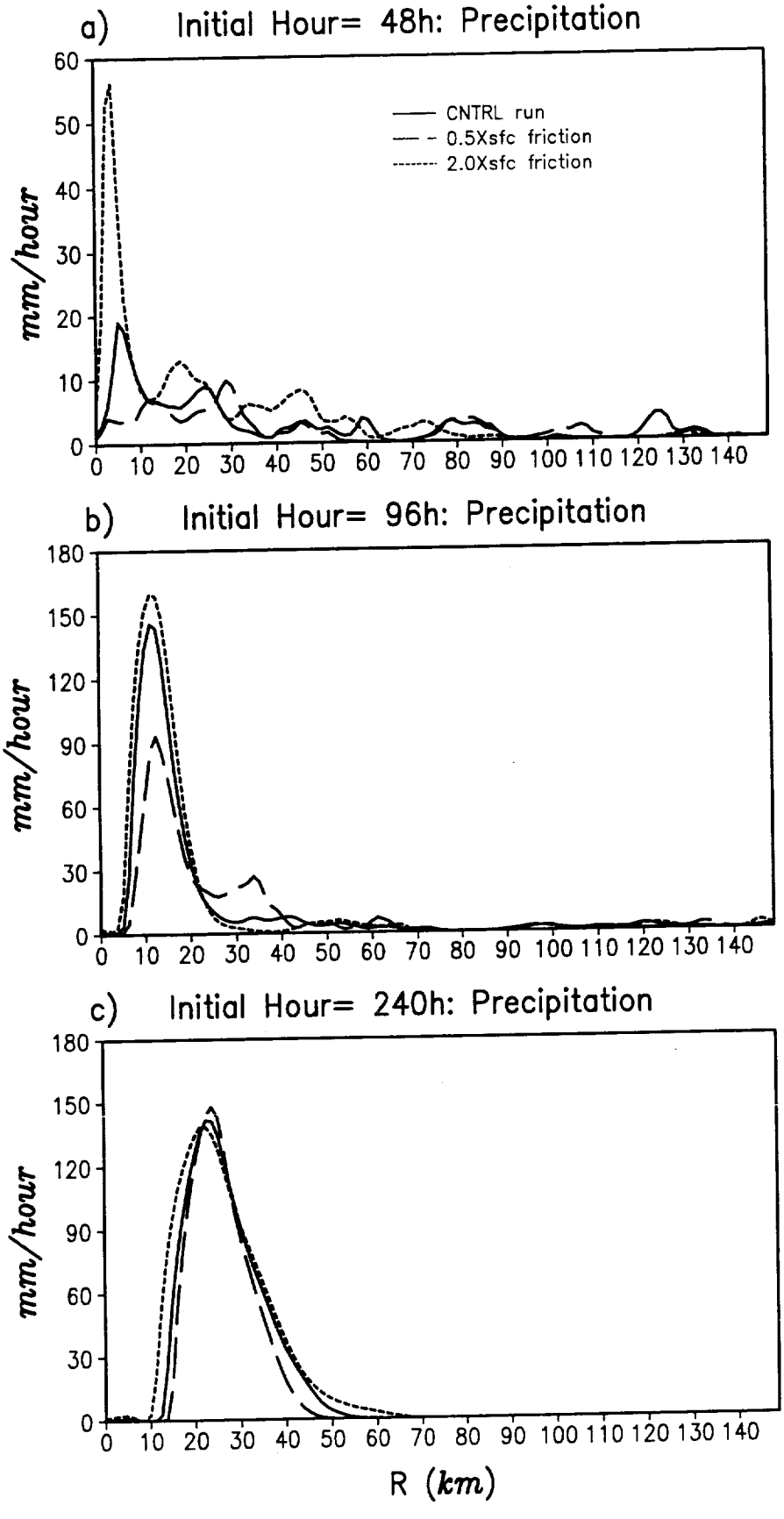
a) Initial Hour= 48h: Precipitation
CNTRL run
0.5Xsfc friction
2.0Xsfc friction
mm/hour
b) Initial Hour= 96h: Precipitation
mm/hour
c) Initial Hour= 240h: Precipitation
mm/hour
R (km)

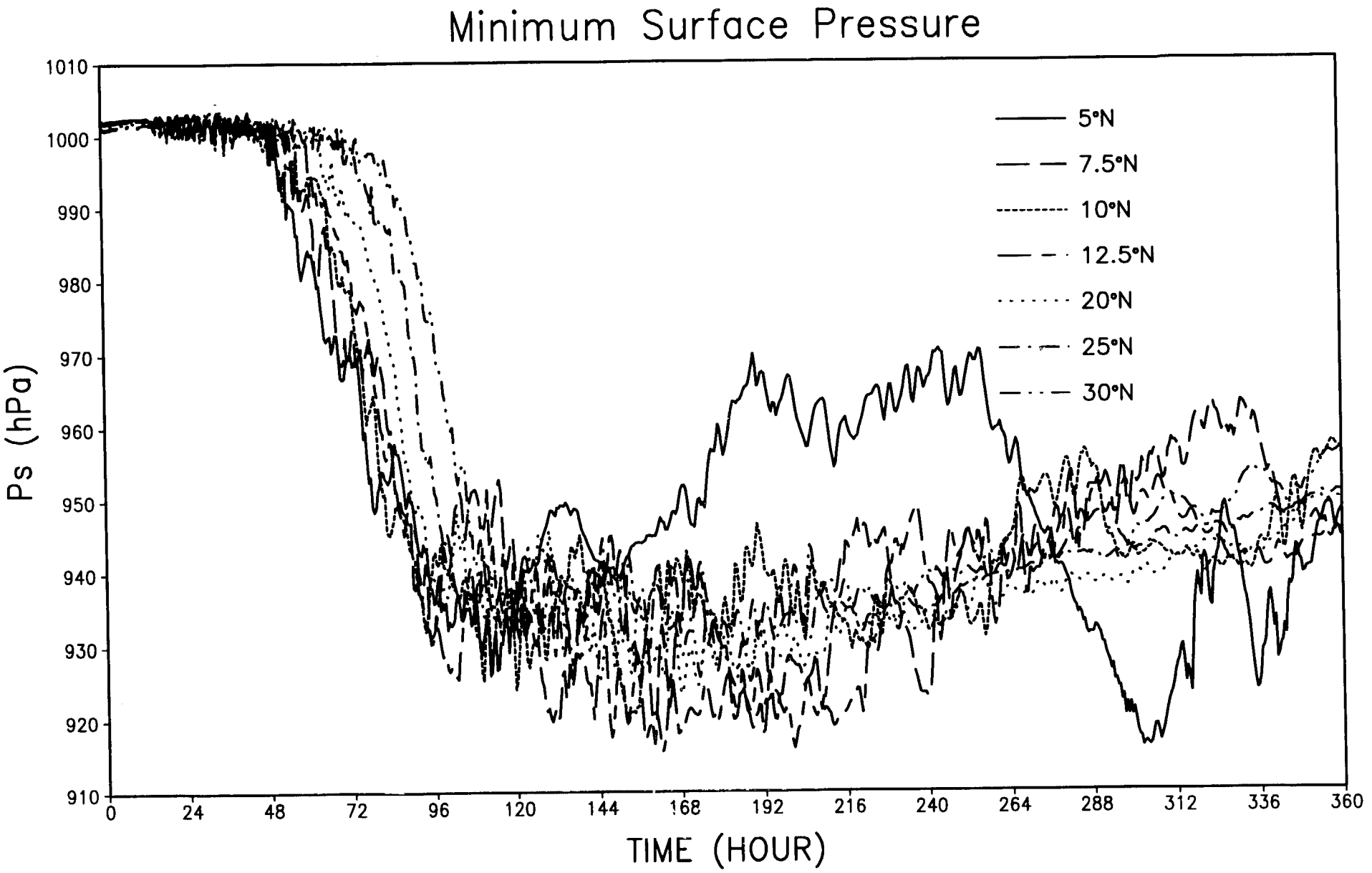
Minimum Surface Pressure
Ps (hPa)
1010
1000
990
980
970
960
950
940
930
920
910
0
24
48
72
96
120
144
168
192
216
240
264
288
312
336
360
TIME (HOUR)
5°N
7.5°N
10°N
12.5°N
20°N
25°N
30°N
Plot created: 07/23/02 14:03:16

6b

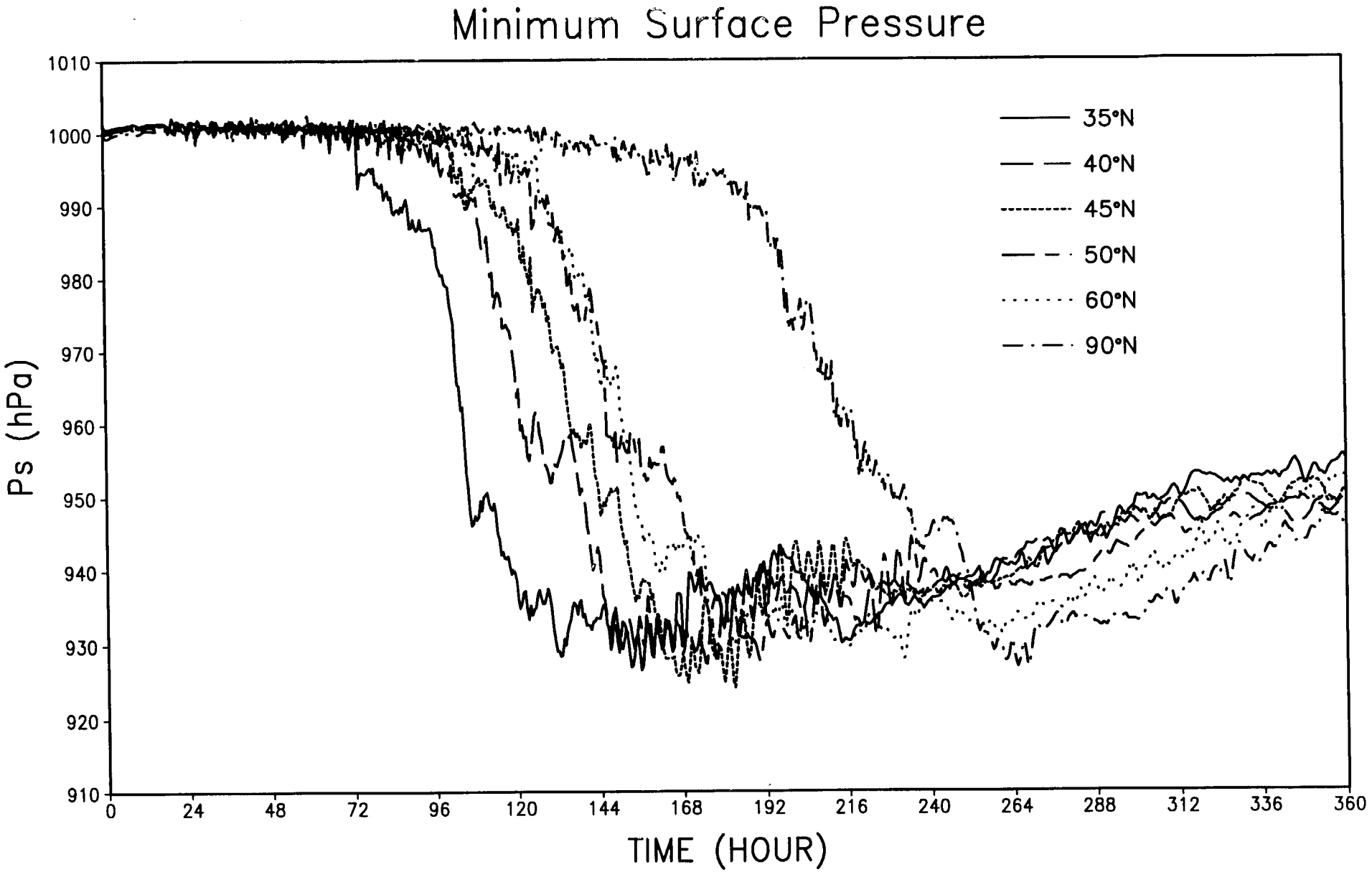
Minimum Surface Pressure
1010
1000
990
980
970
960
950
940
930
920
910
Ps (hPa)
0
24
48
72
96
120
144
168
192
216
240
264
288
312
336
360
TIME (HOUR)
35°N
40°N
45°N
50°N
60°N
90°N
Plot created: 07/23/02 14:01:38

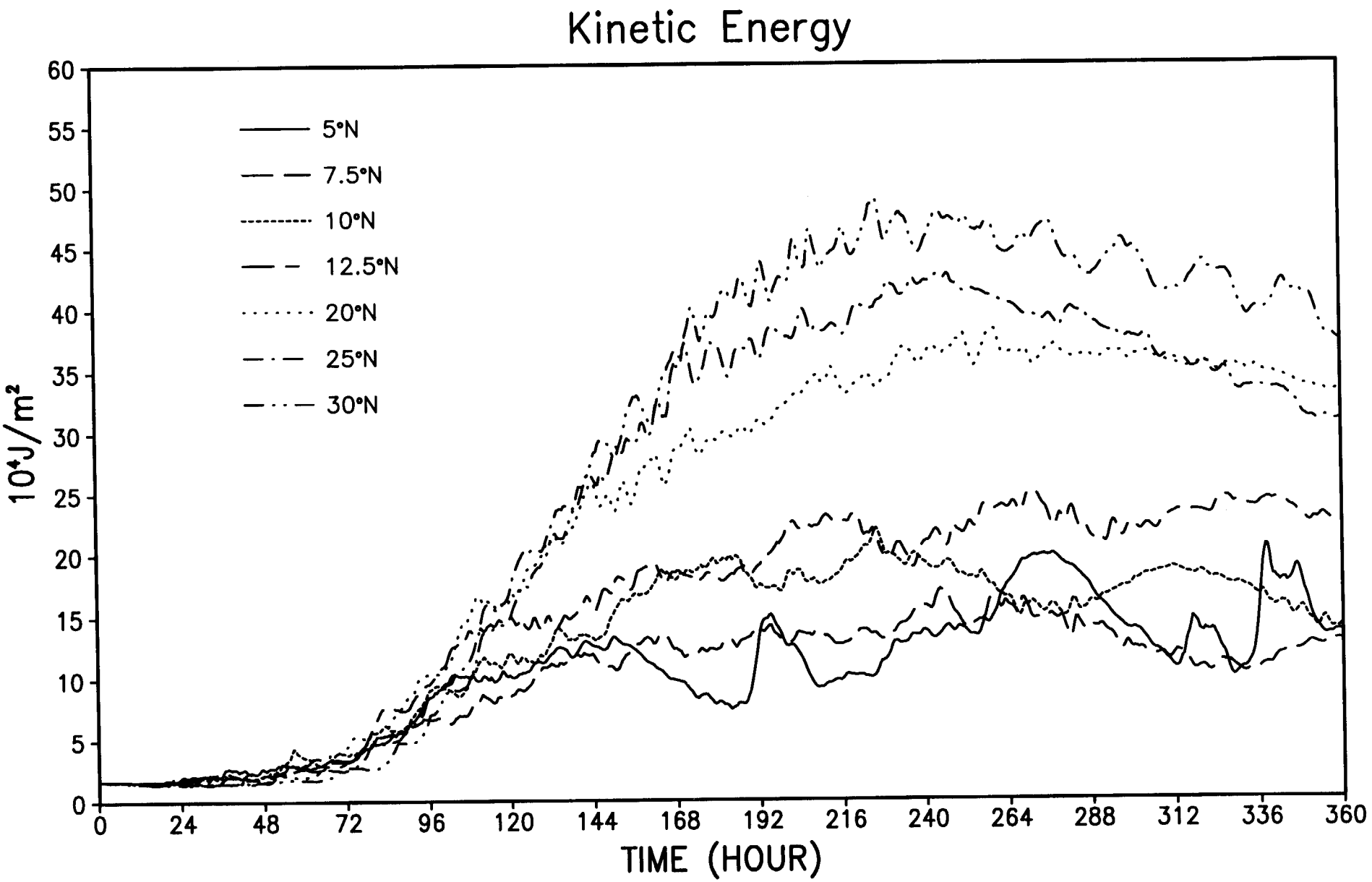
Kinetic Energy
5°N
7.5°N
10°N
12.5°N
20°N
25°N
30°N
10⁴J/m²
0
5
10
15
20
25
30
35
40
45
50
55
60
0
24
48
72
96
120
144
168
192
216
240
264
288
312
336
360
TIME (HOUR)
Plot created: 07/23/02 14:24:14

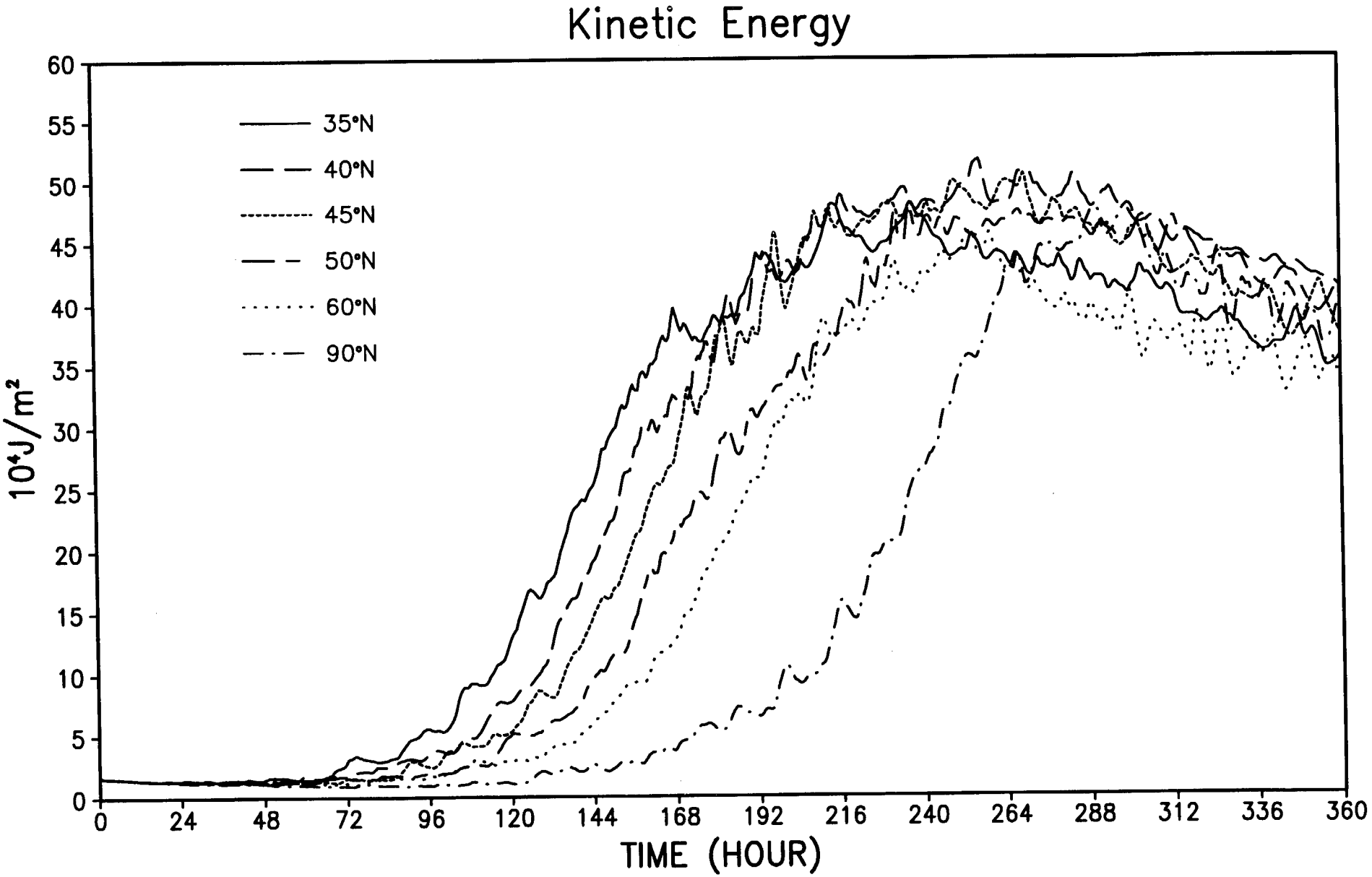
Kinetic Energy
35°N
40°N
45°N
50°N
60°N
90°N
10⁴J/m²
0
5
10
15
20
25
30
35
40
45
50
55
60
0
24
48
72
96
120
144
168
192
216
240
264
288
312
336
360
TIME (HOUR)
Plot created: 07/23/02 14:26:07

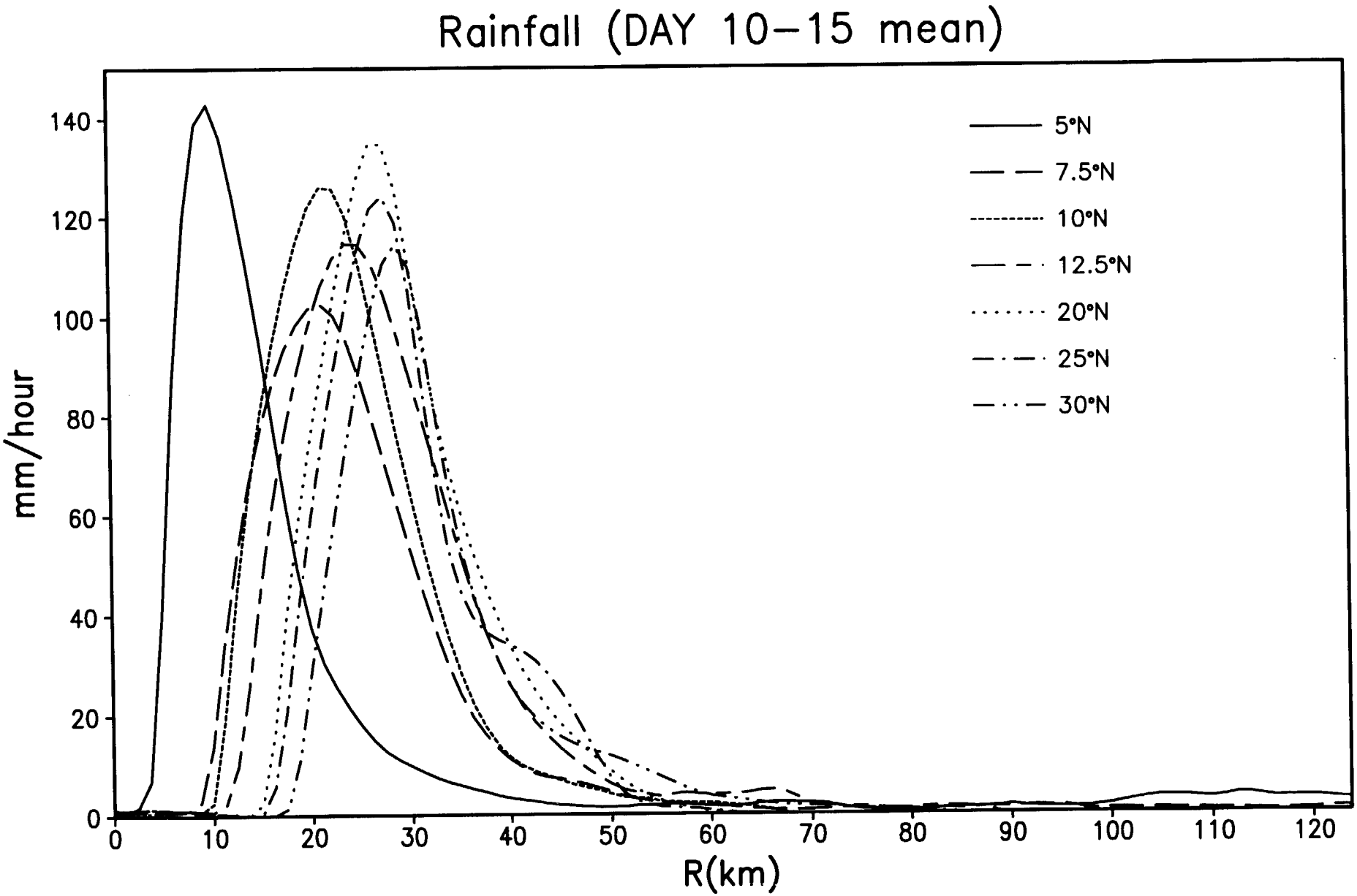
Rainfall (DAY 10–15 mean)
mm/hour
R(km)
5°N
7.5°N
10°N
12.5°N
20°N
25°N
30°N
0
20
40
60
80
100
120
140
0
10
20
30
40
50
60
70
80
90
100
110
120
Plot created: 07/29/02 10:51:14

8.6

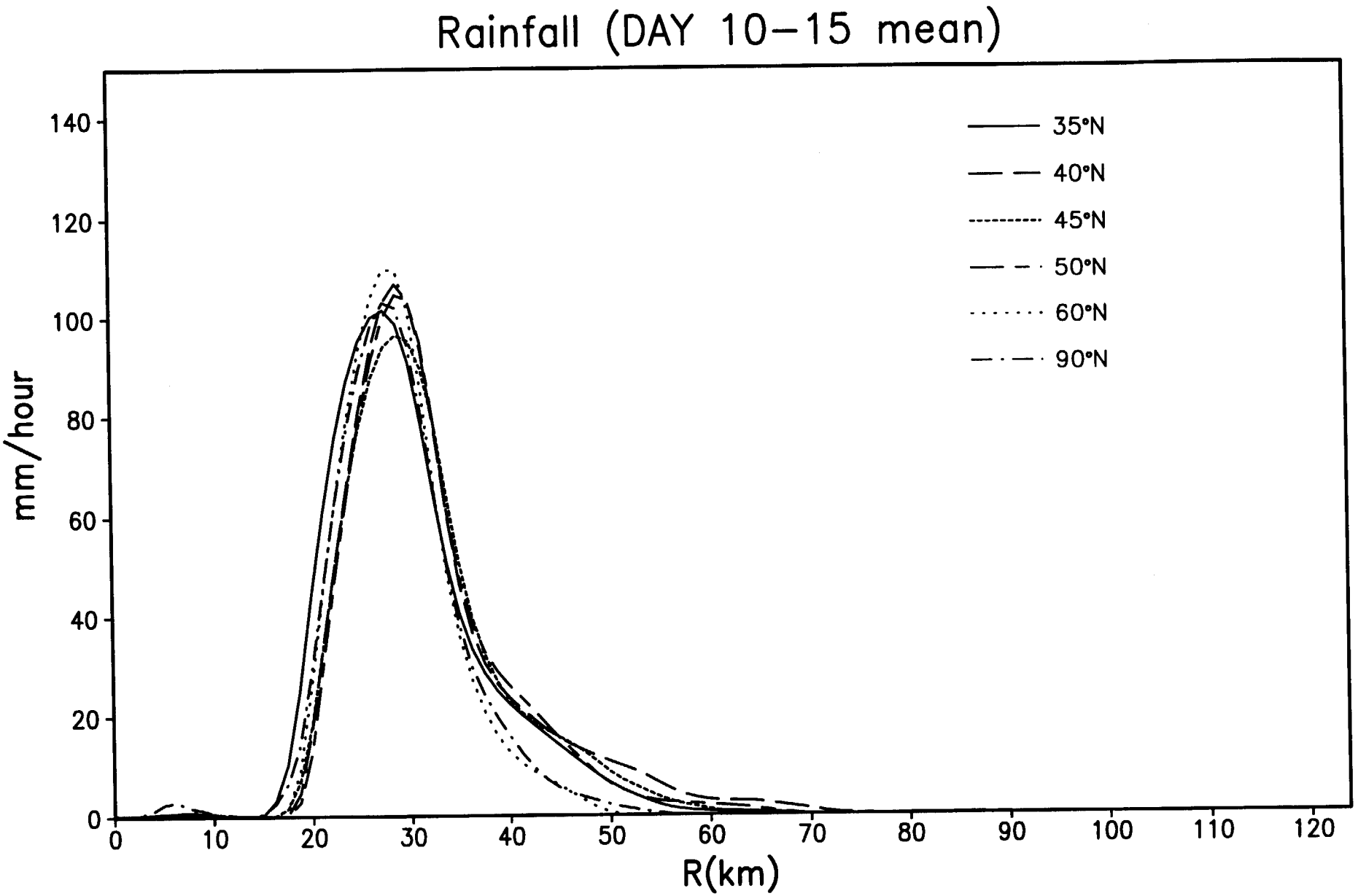
Rainfall (DAY 10–15 mean)
35°N
40°N
45°N
50°N
60°N
90°N
mm/hour
R(km)
0
20
40
60
80
100
120
140
0
10
20
30
40
50
60
70
80
90
100
110
120
Plot created: 07/29/02 10:54:59